ENVIRONMENTAL ENGINEERING SCIENCE
Volume 00, Number 00, 2018

DOI: 10.1089/ees.2017.0263

ORIGINAL ARTICLE

New Biosorbent Based on Al_2O_3 Modified Lignocellulosic Biomass (*Lagenaria vulgaris*): Characterization and Application

Nena Velinov,* Jelena Mitrović, Miljana Radović, Milica Petrović, Miloš Kostić, Danijela Bojić, and Aleksandar Bojić

Department of Chemistry, Faculty of Science and Mathematics, University of Niš, Niš, Serbia.

Received: June 28, 2017 *Accepted in revised form: November 22, 2017*

Abstract

A new biosorbent, obtained by chemical modification of lignocellulosic biomass with Al_2O_3, was tested for removal of anionic surfactant sodium dodecylbenzenesulfonate (DBS) from aqueous solution in batch conditions. As a basic lignocellulosic material for chemical modification by Al_2O_3 was used *Lagenaria vulgaris* shell (LVB). Biosorbent characterization was performed by Fourier transform infrared spectroscopy, scanning electron microscopy with energy dispersive X-ray spectroscopy, and X-ray diffraction analysis. Obtained matter showed significant improvement of removal efficiency compared with unmodified biomass. Effect of initial pH value, biosorbent dosage, and initial concentration of DBS on the sorption process was studied. Sorption of DBS onto LVB-Al_2O_3 was highly pH dependent. Complete DBS removal was attained at lower pHs; as pH increased up to 9, DBS removal rapidly decreased. Optimal sorbent dosage was 2 g/dm^3. Sorption kinetics followed pseudosecond-order, intraparticle diffusion and Chrastil's models, suggesting that both surface reaction and diffusion were rate-limiting steps. Equilibria experimental results were best fit by Langmuir sorption isotherm models. Maximum sorption capacity of LVB-Al_2O_3 for DBS was found to be 513.28 mg/g. The present study suggests that the chemically modified *L. vulgaris* shell with Al_2O_3 could be used effectively for the removal of DBS from aqueous solution.

Keywords: Al2O3; biomaterial; modification; sodium dodecylbenzenesulfonate; sorption; wastewater treatment

Introduction

Surfactants are synthetic organic chemicals used in high volumes in detergents, personal care, and household cleaning products, which may act as detergents, wetting agents, emulsifiers, foaming agents, and dispersants (Kosswig, 2006). Surfactants are usually classified according to the polar head group. One of the most common groups of surfactants is linear alkyl benzene sulfonate, with a typical representative sodium dodecylbenzenesulfonate (DBS), which is a major component of laundry detergents. Millions of kilograms of surfactants are produced annually so that they are released into the environment in large quantity (Rosen and Kunjappu, 2012; Jardak *et al.*, 2016). Surfactants are harmful to both terrestrial and aquatic life.

Moreover, surfactants persist in biota for long time periods (Cserháti *et al.*, 2002). When present above a certain concentration in water, surfactants reduce the quality of water, impart unpleasant taste and odor, cause foams in rivers and effluent treatment plants, and cause both short- and long-term changes in the ecosystem. By reducing the surface tension of water, surfactants allow easy *in vivo* penetration of aqueous solutions and thus affect aquatic life adversely. It has also been shown that surfactants can potentially act synergistically with other toxic chemicals present in natural waters (Lewis, 1991; Mösche and Meyer, 2002; Ying, 2006).

Among various processes adopted for surfactant removal, biosorption is a promising alternative technology, using inactive and dead biomasses as sorbents, with the advantages of low cost, availability in nature, greater profitability, and ease of operation. Biosorbents are inexhaustible, low-cost, and nonhazardous materials, which require easy processing. Different plant lignocellulose biomasses (orange peels, sugar cane bagasse, coconut shells, olive stones, olive tree prunings, cabbage waste, banana peels, and cashew bagasse) are commonly used as biosorbents for synthetic and real wastewater treatment, which are typically composed of cellulose, hemicellulose, and lignin (Abdolali *et al.*, 2014; Bhatnagar *et al.*, 2015; De Quadros Melo *et al.*, 2016; Kumar *et al.*, 2017).

Biomaterials can be chemically modified by inorganic materials, such as metal oxides, providing new, unique hybrid, or

**Corresponding author:* Department of Chemistry, Faculty of Science and Mathematics, University of Niš, 33 Višegradska Street, Niš 18000, Serbia. *Phone:* +381 69 4220600; *Fax:* +381 18 533014; *E-mail:* nena.velinov@yahoo.com

composite materials (Bakircioglu *et al.*, 2010; Copello *et al.*, 2011; Liu *et al.*, 2011; Mahmoodi *et al.*, 2011). Modifications of biosorbents by metal oxides may improve their sorption characteristics, mechanical properties, and ability to remove many organic pollutants, which could not be effectively removed from water with starting biomaterial.

In this article, to get a chemically modified biosorbent as a basic lignocellulosic material was used *Lagenaria vulgaris* shell. *L. vulgaris* is a large annual herb that can be grown worldwide. It is mostly composed of cellulose and lignin (Shah *et al.*, 2010). *L. vulgaris* shell possesses a macroporous structure, very high mechanical stability under various biosorption treatment conditions, it does not swell in water, and its lignocellulosic structure offers the possibility of chemical modification (Stanković *et al.*, 2013). In addition, it is easily available, environmentally friendly, inexpensive, and easy to grow and prepare.

Biosorbents based on *L. vulgaris* shell and biosorbents obtained by its modifications have been used predominantly for efficient removal of metal cations from water (Mitic-Stojanovic *et al.*, 2011; Stanković *et al.*, 2013; Kostić *et al.*, 2014). In an attempt to improve *L. vulgaris* biosorbent to remove not only metal cations but also organic pollutants from water, a new biosorbent based on chemical modification by a small amount of Al_2O_3, was synthesized.

In this article, the synthesis, characterization, and application of a novel *L. vulgaris*-Al_2O_3 biosorbent for the removal of DBS from aqueous solution was studied. The effect of initial pH value, initial concentration of DBS, and biosorbent dosage on DBS removal was examined. Biosorbent characterization was performed by Fourier transform infrared spectroscopy (FTIR), scanning electron microscopy with energy dispersive X-ray spectroscopy (SEM-EDX), and X-ray diffraction (XRD). Four kinetic models (pseudofirst-order, pseudosecond-order, intraparticle diffusion, and Chrastil's model) were used to determine the kinetic parameters. The experimental results were fitted to the Langmuir, Freundlich, and Dubinin–Radushkevich isotherm models.

Materials and Methods

Sodium salt of DBS was purchased from Sigma-Aldrich, and $Al(NO_3)_3 \times 9H_2O$, HNO_3 and NaOH were of reagent grade (Merck, Germany). All chemicals were used without further purification. All solutions were prepared with deionized water (18 MΩ). The main characteristics of DBS are shown in Table 1 in Supplementary Data.

Preparation of biosorbent

Experiments were performed using a shell of *L. vulgaris*, which was roughly crushed, washed with deionized water, and ground by laboratory mill. Biomass was acid treated (0.3 M HNO_3) to remove bioaccumulated metals, then alkali treated (1 M NaOH) in the period of 60 min. Ten grams of obtained material was dispersed in 100 cm^{-3} of solution containing 1 g of $Al(NO_3)_3 \times 9H_2O$ and the dispersion was stirred for 0.5 h at 25.0°C ± 0.5°C. After that the solution was evaporated. The obtained material was washed with deionized water, treated by trimethylamine, then washed with deionized water until neutral pH, and dried at 55°C ± 1°C for 5 h. This material was abbreviated as LVB- Al_2O_3.

Characterization of biosorbent

Content of Al in the biosorbent was determined using the inductively coupled plasma optical emission spectrometry (ICP-OES) model iCAP 6500 Duo (Thermo Scientific, United Kingdom) equipped with a CID86 chip detector. SEM was performed using the JEOL JSM −5300 equipped with EDS LINK QX 2000 ANALYTICAL. For SEM-EDX analysis, samples were attached to aluminum stubs using Leit-C carbon cement. A JEOL SEM in low-vacuum mode was used for imaging the samples with an Oxford Instruments X-MAX 50 cm3 detector for semiquantitative EDX analysis. Nominal magnifications of $\times 50, \times 100$, and $\times 200$ were used when imaging the samples. Three random particles averaged for EDX analysis.

FTIR spectra were recorded by means of BOMEM MB-100 FTIR spectrometer (Hartmann & Braun, Canada) using KBr pellets containing 1.0 mg of the sample in 150 mg KBr. Instrument is equipped with a standard DTGS/KBr detector in the range of 4000–400 cm^{-1} with a resolution of 2 cm^{-1}. Crystal structure was analyzed by XRD using filtered Cu Kα radiation (Ultima IV Rigaku). The experiments were performed in the scan range $2\theta = 5$–90° under 40 kV, 40 mA, with scan speed 5 degree/min and steps with 0.02 degree. Before measurement, the angular correction was done by high-quality Si standard. Lattice parameters were refined from the data using the least square procedure. Standard deviation was about 1%.

Suspension pH (pH_{sus}) relates to the overall acidity or basicity of the adsorbent. In the present study, biosorbent samples (0.2 g) were suspended into 50 mL of deionized water and equilibrated for 24 h. The resulting pH was denoted as pH_{sus}. The point of zero charge was determined by the pH drift method (Yang *et al.*, 2004) with some modifications for LVB-Al_2O_3. The pH of test solutions was adjusted in the range between 2 and 10 using 0.01 M HNO_3 and 0.01 M KOH. Biosorbent samples (0.2 g) were added to 50 mL of test solutions into stopped glass tubes and equilibrated for 24 h. The final pH (pH_f) was measured after 24 h and plotted against the initial pH (pH_i). The pH at which the curve crosses the line $pH_i = pH_f$ was taken as pH_{pzc}.

Oxygen acidic functional groups in LVB-Al_2O_3 were determined by potentiometric titration based on Boehm's method (Boehm, 1966; Goertzen *et al.*, 2010). This method is based on the titration of functional groups with different acidity constants using base solutions of increasing strength ($NaHCO_3$, Na_2CO_3, and NaOH). Solutions of bases were freshly prepared and stored in nitrogen atmosphere. First, each biosorbent was protonated with 0.01 M HCl and dried at 50°C. Then, protonated biosorbent (0.5 g) was suspended in 50 mL of 0.1 M $NaNO_3$. To achieve equilibrium, the suspension was stirred on a magnetic stirrer for 1.5 h before titration. Increments of base (0.04–0.06 mL) were successively added. The next increment was added after reaching equilibrium. One hour before and during the titration, nitrogen gas was bubbled through the solution to avoid dissolution of carbon dioxide.

Batch sorption experiments

Working model solutions were prepared by the appropriate dilution of the stock solutions (1.0000 g/dm^3). The pH of the solutions was adjusted with 0.1/0.01 mol/dm^3 NaOH/HNO_3

solutions pH metrically (SensIon5; HACH). All experiments were performed at 25.0°C ± 0.2°C. The aliquots of the solution were taken before the sorption started and after particular periods of time. DBS concentration was determined using the methylene blue active substances assay (MBAS assay) (George and White, 1999). MBAS assay is a photometric analysis test method that uses methylene blue to determine the presence of anionic surfactants. The limit of detection for this version of the method is ~0.1 ppm (Eaton *et al.*, 1998). The amount of adsorbed DBS q_t (mg/g) was determined by using the following equation:

$$q_t = \frac{(c_0 - c_t)V}{m_b} \quad (1)$$

where c_0 and c_t are the initial and final DBS concentrations (mg/dm^3), V is the solution volume (dm^3), and m is the mass of the sorbent (g).

The removal efficiency (RE) of DBS by biosorbent was calculated using the following equation:

$$\mathrm{RE}(\%) = \frac{c_0 - c_t}{c_0} \times 100 \quad (2)$$

In all experiments, solution samples were taken in triplicate for the measurement of metal ion concentrations. Average values ± SD (error bars) are presented in all graphs and tables. All the kinetics and isotherm parameters were evaluated with the nonlinear regression method by means of Origin Pro 2016 software.

Results and Discussion

Material characterization

Physicochemical characteristics of LVB-Al_2O_3 biosorbent are shown in Table 1.

SEM images of LVB and LVB-Al_2O_3 (Fig. 1) show a porous morphology of the biomaterial. The surface structure of the biomaterial before (Fig. 1a–c) and after incorporation of Al_2O_3 (Fig. 1d–f) is very similar, meaning that the modification process did not bring any significant change of morphological structure of the biomaterial surface. The surface of the LVB-Al_2O_3 biosorbent is smooth, with characteristic channels and macropores, like those of basic material LVB (Mitic-Stojanovic *et al.*, 2011). The sample had particle sizes above 1 mm and consisted of cell-like structures of around 100 μm in size. These structures have holes of around 1 μm in a random position over the cell-like units. Visible Al_2O_3 layers, particles, and/or ''islands'' as the separate phase on the biomaterial surface were not detected. These indicated that Al_2O_3 was highly and homogeneously dispersed, without a change in the biomaterial structure.

Table 1. Physicochemical Characteristics of LVB-Al_2O_3 Biosorbent

Parameter	*Value*
Al_2O_3 content in LVB-Al_2O_3	17.48%
pH_{sus}	5.93
pH_{PZC}	5.85
Acidic functional groups by Boehm titrations	
Carboxylic groups (mmol/g)	0.2081
Lactonic groups (mmol/g)	0.0366
Phenolic groups (mmol/g)	0.0096

LVB-Al_2O_3, *Lagenaria vulgaris*-Al_2O_3 biosorbent.

EDX analysis (Fig. 2) shows the presence of carbon and oxygen in unmodified biomass (Fig. 2a) and carbon and oxygen with aluminum in LVB-Al_2O_3 biosorbent (Fig. 2b). Base on weight percentage quantification of samples, there is 57.38% of carbon and 42.62% of oxygen in biomaterial before modification and 29.63% of carbon, 52.87% of oxygen, and 17.50% of aluminum in LVB-Al_2O_3 biosorbent. The content of aluminum in the LVB-Al_2O_3 biosorbent is in agreement with the results obtained by the ICP-OES method (Table 1).

FTIR spectrum of the chemically modified LVB is shown in Fig. 3. Modification of the LVB biomass by Al_2O_3 generated several changes in the IR region of 4,000–400 cm^{-1}. First, there is a slight displacement of the band associated to the O-H deformation mode, from 1,635 to 1,641 cm^{-1}. The increase in intensity of the band at around 1,458 cm^{-1} may be associated with the interaction or coordination between aluminum and carboxyl groups from components of lignocellulosic biomass (Benítez-Guerrero *et al.*, 2014). It has been reported that the symmetrical COO- stretching vibrations corresponding to carboxylate bridges established with aluminum centers of different nature are located between 1,470 and 1,460 cm^{-1} (Landry *et al.*, 1995; Van den Brand *et al.*, 2004).

Second, changes attributed to the degradation and removal of some lignocellulosic components, as well as to the decomposition of carbohydrates during the reaction and alumina infiltration period in appropriate medium and under certain reaction conditions (pH, T). The band at 1,732 cm^{-1} that is observed in the spectrum of the untreated LVB is involved either to the acetyl and uronic ester groups of the hemicellulose or to the carboxylic group of the ferulic and p-coumaric acids of lignin and hemicellulose (Elanthikkal *et al.*, 2010). Probably the clear peak represents the C = O stretching vibration, which may originate from nonionic carboxyl groups (−COOH or $-COOCH_3$), and may be assigned to carboxylic acids or corresponding esters presented in the hemicellulose or lignin. This peak is weak in the case of unmodified biomass spectrum and disappears in spectra of modified LVB, confirming the fact that carboxyl groups of lignin from unmodified biomass are mostly in ionic form due to hydrolysis of −COOR and ionization of −COOH, indicating a partial removal of lignin.

Moreover, in the FTIR spectra of modified LVB (Fig. 3), the absorption band from O-H stretching vibration moved to higher wave numbers, from 3,424 to 3,441 cm^{-1}, indicating the broken inter- and intramolecular hydrogen bonds in cellulose. This finding indicates that the -OH groups can be involved in the sorption process. The OH groups of cellulose types can rotate and orient themselves to make interactions with adjacent groups of alumina. Furthermore, FTIR spectrum of modified LVB biosorbent showed that the peaks originating from C-O stretching vibration of cellulose expected at 1,052, 1,109, and 1,158 cm^{-1} were shifted to 1,056, 1,116, and 1,161 cm^{-1}, respectively. This finding indicates that the hydroxyl groups were involved in aluminum interaction. These groups present in the biomass may act in deprotonated forms as key sites in coordination of metals.

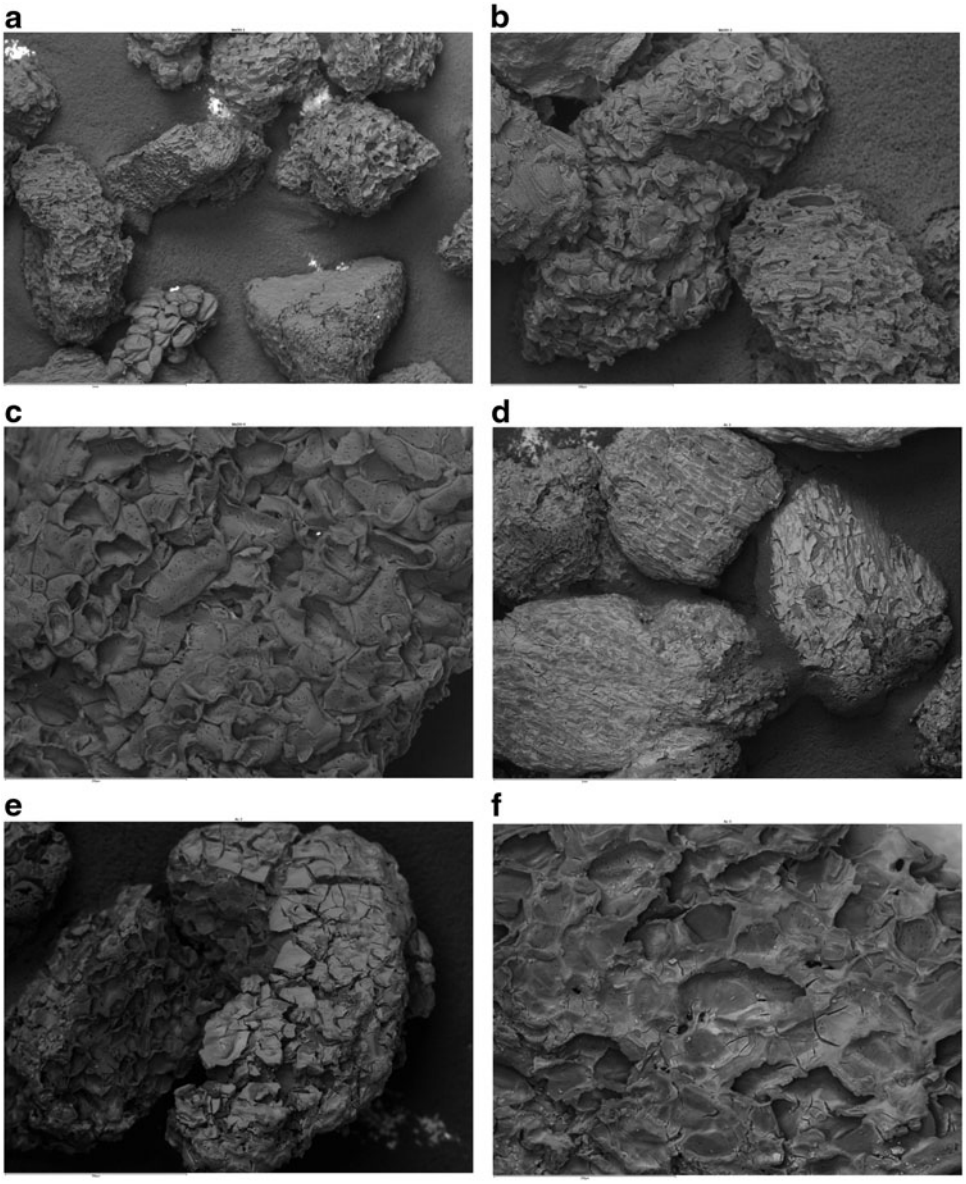

FIG. 1. SEM images of unmodified biomass at a magnification of **(a)** × 50, **(b)** × 100, and **(c)** × 200 and of LVB-Al_2O_3 biosorbent at magnification of **(d)** × 50, **(e)** × 100, and **(f)** × 200. LVB-Al_2O_3, *Lagenaria vulgaris*-Al_2O_3 biosorbent.

When the lignocellulose biomass reacted with alumina, the FTIR spectrum of modified LVB showed a considerable decrease in the intensity of the band at 1,335 cm^{-1} originating from O−H in plane bending vibration, and the appearance of a new intensive band at 1,317 cm^{-1} typical for C−H wagging vibrations of the CH_2 groups, confirming that alumina molecules are coupled to the surface of cellulose chains. In addition, distinct changes in the FTIR spectrum of the modified biosorbent are noted in the region 800–400 cm^{-1}. The O−H out of plane bending vibrations in this area has a higher absorbance intensity ratio for higher substituted samples (El-Sakhawy, 2001). This area indicates a higher occupation of the alumina octahedral sites, corresponding to Al-O vibration. These sites have a higher coordination and their occupation will be favored by specified synthesis.

The XRD pattern of LVB-Al_2O_3 shows the peaks that are typical for lignocellulosic materials with amorphous regions (Fig. 1 in Supplementary Data). The XRD pattern of LVB-Al_2O_3 does not contain any characteristic peak of Al_2O_3, which appears in the XRD spectra of different crystalline alumina (Kumar *et al.*, 1999). Obtained XRD results mean that Al_2O_3 does not exhibit its individual characteristics, even though its presence in the material was confirmed.

Results of the XRD analysis of LVB-Al_2O_3 are in accordance with the result obtained by SEM-EDX analysis, which did not detect Al_2O_3 as a separate phase on the biosorbent surface. It can be assumed that LVB-Al_2O_3 is a unique, highly amorphous lignocellulosic material, where Al_2O_3 is bound to a biomass. This fact, as well as its absorption bands presented in the FTIR spectrum of LVB-Al_2O_3, indicates that it is chemically bonded to the biomaterial functional groups creating new specific active centers.

The pH of LVB-Al_2O_3 biosorbent suspension in demineralized water (pH_{sus}) was 5.93 probably due to the presence of surface acidic groups. The point of zero charge (pH_{pzc}) of LVB-Al_2O_3 was 5.85, which means that at pH lower than 5.85, its surface is positively charged and at pH higher than 5.85, it is negatively charged. The pH_{pzc} of not modified LVB was 6.10, meaning that the modification made the material a little more acidic (Mitic-Stojanovic *et al.*, 2011).

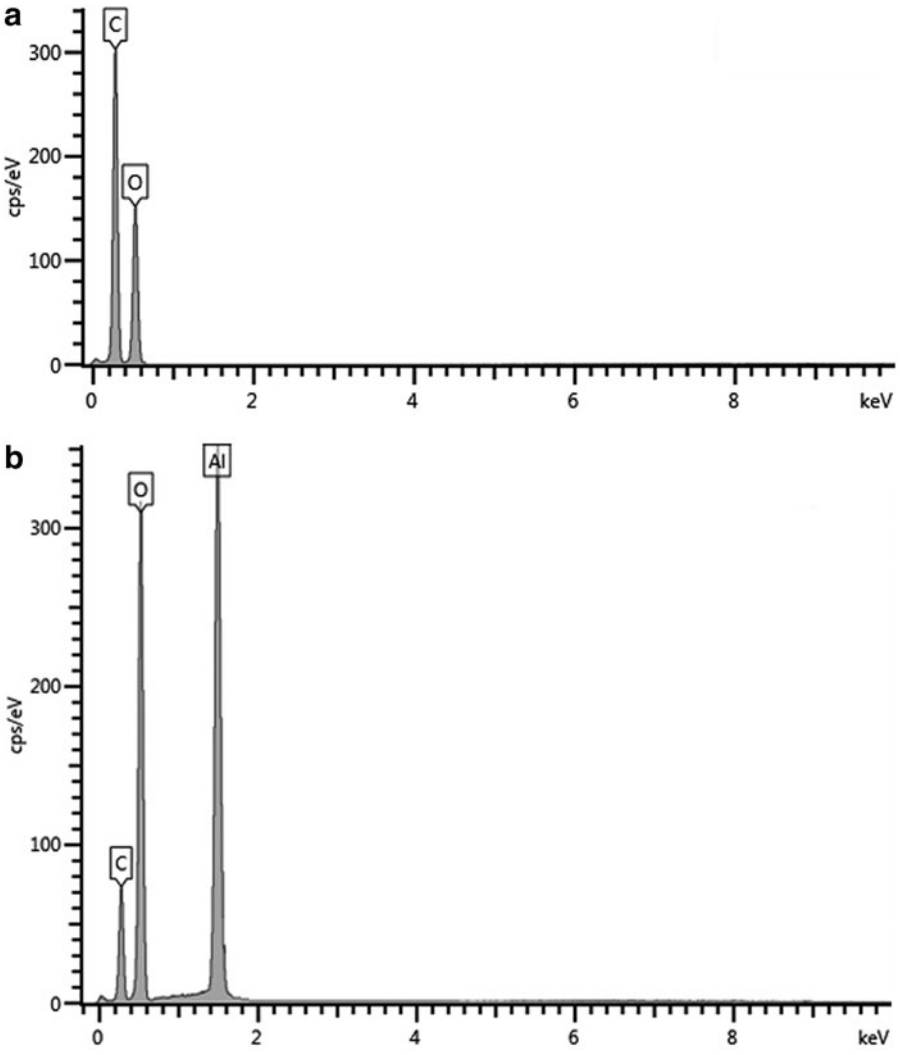

FIG. 2. EDX spectrum of **(a)** unmodified biomass and **(b)** LVB-Al_2O_3 biosorbent.

Based on Boehm's analysis, the amount of acidic groups was calculated assuming that NaOH neutralizes carboxylic, phenolic, and lactonic groups; Na_2CO_3 neutralizes carboxylic and lactonic groups, while $NaHCO_3$ neutralizes only carboxylic groups. The total content of acidic functional groups at LVB-Al_2O_3 surface, determined by titration with NaOH as a reagent, was calculated to be 0.2352 mmol/g. The content of carboxyl groups, as strongly acidic functional groups, was 0.2081 mmol/g. The concentrations of lactones and phenols determined for LVB were 0.0366 and 0.0096 mmol/g, respectively. Biosorbent LVB-Al_2O_3 has fewer amounts of acidic groups than LVB (Mitic-Stojanovic *et al.*, 2011).

This indicated that chemical modification with Al_2O_3 decreases the contribution of oxygen functional groups in biosorbent, probably because they are replaced with new functional groups, creating a new specific active center for substrate binding. However, the remaining acidic functional groups on LVB-Al_2O_3 probably also participate in the binding mechanism for the sorption of DBS.

Effect of initial pH

Removal of DBS by LVB-Al_2O_3 is significantly affected by the pH value of the solution, thereby changing the surface charge of the sorbent and charge of sulfonic group in DBS molecules. The experiments were studied by varying initial pH value from 1.0 up to 9.0, while other parameters were kept constant (initial DBS concentration 40.0 mg/dm^3, sorbent dose 2.0 g/dm^3, temperature 25.0°C ± 0.2°C). Results show that an increase in the solution pH from 1 to 9 led to a decrease of RE of DBS (Fig. 4).

DBS has a sulfonic group, which is negatively charged even at lower pH, because its pKa value is lower than zero (Roberts and Caserio, 1977). The biosorbent surface has many different functional groups and its net charge is pH dependent, especially because of the presence of the –C–O–Al–$(OH)_2$ group. At pH values lower than pH_{pzc}, this group is protonated and the sorbent surface is positively charged. It can be assumed that the main binding mechanism is ionic exchange, based on the attraction between negatively charged sulfonic group of DBS and the positively charged sorbent surface.

With the increasing medium pH, the net positive charge of the surface decreases and the DBS uptake decreases as well. At pHs higher than pH_{pzc}, the sorbent surface becomes negatively charged, the DBS binding rapidly decreases, reaching its minimum at pH 9, and remaining constant with further increase of pH (Guerrero-Coronilla *et al.*, 2015; Albadarin *et al.*, 2017). However, at higher pH values, the

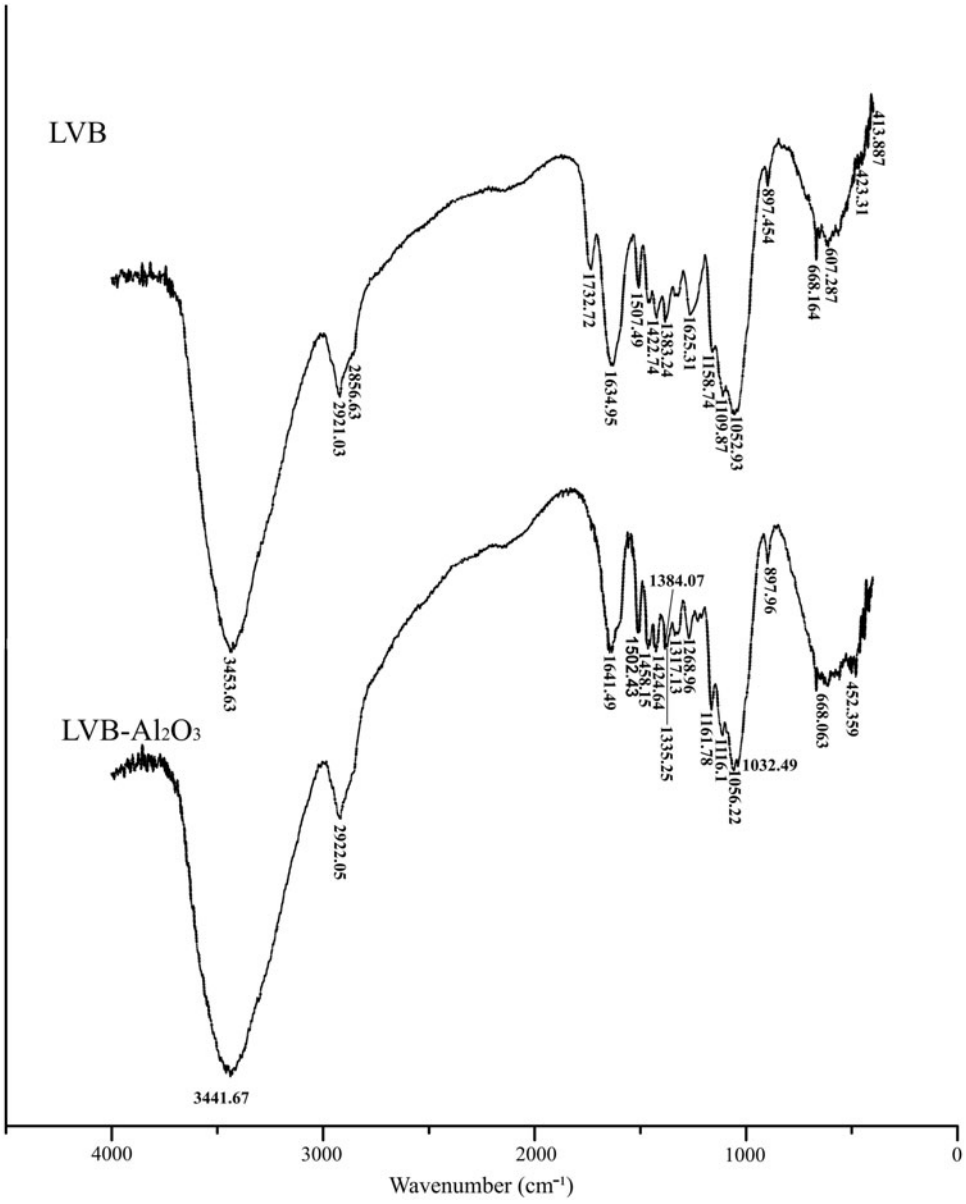

FIG. 3. FTIR spectra of unmodified biomass and LVB-Al_2O_3. FTIR, Fourier transform infrared spectroscopy.

material has adsorbed a certain amount of DBS as well, indicating that ionic exchange is not the only sorption mechanism, although it is predominant. The effect of pH on the sorption of DBS on LVB-Al_2O_3 is similar to that reported in the literature for the sorption of DBS by sand sorbents (Khan and Zareen, 2006) and by metal oxide modified biomaterials (Copello *et al.*, 2011; Mahmoodi *et al.*, 2011).

Effect of sorbent dosage

Effect of sorbent dose on DBS RE was investigated at LVB-Al_2O_3 doses ranging from 0.5 to 8.0 g/dm^3. The results are presented in Fig. 5. RE of DBS increased quickly from 73.3% to 99.8% by an increase in the sorbent dose from 0.5 to 2 g/dm^3, because of the increased active surface area of the biosorbent and the number of available binding sites for DBS. Further increasing of the sorbent dose to 4 g/dm^3 slightly enhanced RE to 99.9%. RE was almost without change at the sorbent doses of 6.0 and 8.0 g/dm^3.

A negligible change of the RE at biosorbent dosage higher than 2.0 g/dm^3 may be attributed to the presence of the excess of active centers for DBS binding on biosorbent surface, with regard to the amount of DBS molecules at applied initial concentration, suggesting that after a certain dose of sorbent, the maximum sorption is attained and the amount of DBS molecules bound to the sorbent and the amount of free DBS molecules remains constant even with further addition of the dose of sorbent. Therefore, value of 2.0 g/dm^3 was considered as the optimal biosorbent dose of LVB-Al_2O_3 for DBS removal. A similar effect was reported by other authors (Beltrán-Heredia *et al.*, 2012; Bozbas and Boz, 2016; Tural *et al.*, 2017).

Effects of initial DBS concentration

Effects of initial DBS concentration on the RE were investigated at initial DBS concentrations ranging from 10 to 1,200 mg/dm^3 with 2 g/dm^3 biosorbent dosage (Fig. 6). For

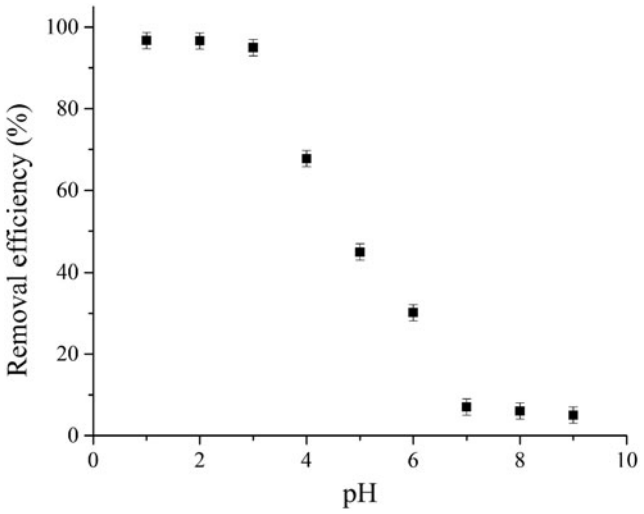

FIG. 4. Effect of pH on DBS removal with LVB-Al_2O_3. Initial DBS concentration 40.0 mg/dm^3, sorbent dose 2.0 g/dm^3, and temperature 25.0°C ± 0.2°C. DBS, sodium dodecylbenzenesulfonate.

the initial DBS concentration of 10 and 20 mg/dm^3, the RE was very high, 99.6 and 98.1%, respectively. At initial concentrations of 50 and 100 mg/dm^3, the RE was still over 90%, but it slowly decreased. With a further increase of initial concentrations from 200 to 600 mg/dm^3, RE exceeded 80%. Removal (%) sharply decreased to 61.88% for the initial DBS concentration of 800 mg/dm^3, and to 56.44% for 1,000 mg/dm^3 of the DBS. For initial concentrations of 1,200 mg/dm^3, removal (%) was very low, 32.51%.

In the case of lower investigated concentrations (10, 20, 50, 100 mg/dm^3), the ratio of initial number of DBS to the available sorption sites is low and the biosorption becomes independent of initial concentration, which enabled the over 90% DBS uptake. At higher investigated concentrations (200, 300, 400, 600, 800, 1,000, 1,200 mg/dm^3), a certain amount of DBS is left unabsorbed in the solution due to a saturation of

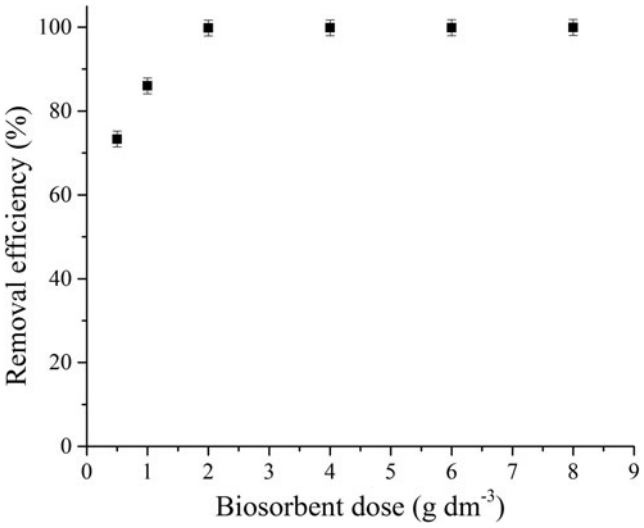

FIG. 5. Effect of sorbent dose on DBS removal with LVB-Al_2O_3. Initial DBS concentration 40.0 mg/dm^3, pH 2.0 ± 0.1, and temperature 25.0°C ± 0.2°C.

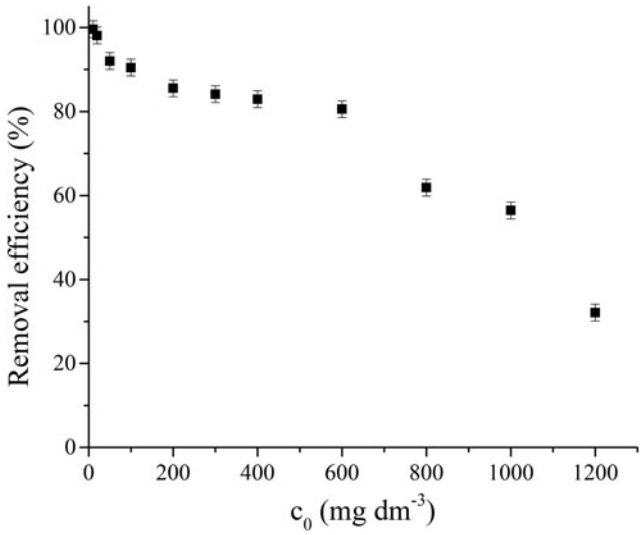

FIG. 6. Effect of initial DBS concentration on the biosorption of DBS onto LVB-Al_2O_3. pH 2.0 ± 0.1, sorbent dose 2.0 g/dm^3, and temperature 25.0°C ± 0.2°C.

the limited available binding sites in the biomass. In that case, the removal of DBS depends on its initial concentration (Beltrán-Heredia *et al.*, 2012; Tural *et al.*, 2017).

However, the biosorption capacity of DBS increases with increasing initial DBS concentration (Fig. 2 in Supplementary Data) and reaches 454.89 ± 6.82 mg/g with 1,200 mg/dm^3 initial concentration of DBS and 2 g/dm^3 dose of biosorbent. This can be attributed to the fact that the higher DBS concentrations increase the overall mass transfer driving force, and thus, the DBS uptakes onto the biosorbent (Liu *et al.*, 2013)

Sorption kinetics

Kinetics of DBS sorption on LVB-Al_2O_3 can be described by the pseudofirst-order model, pseudosecond-order model, intraparticle diffusion kinetic model, and Chrastil's diffusion model.

Pseudofirst-order model. A pseudofirst-order kinetic model describes the rate of sorption, which is proportional to the number of unoccupied binding sites of the sorbent (Lagergren, 1898). It can be expressed in the following form:

$$\frac{dq_t}{dt} = k_1(q_e - q_t) \tag{3}$$

Given the boundary conditions for $t = 0$, $q_t = 0$; $t = t$, $q_t = q_t$, the equation can be integrated to give a nonlinear function:

$$q_t = q_e(1 - e^{k_1 t}) \tag{4}$$

where k_1 (min^{-1}) is the first-order rate constant, q_t and q_e (mg/g) are the amounts of DBS sorbed at time t and at equilibrium, respectively. Plot of q_t versus t for different initial DBS concentrations is shown in Fig. 3 in Supplementary Data.

Pseudofirst-order rate constant k_1 and the predicted q_e values by nonlinear analysis are given in Table 2. As can be

TABLE 2. VALUES OF KINETIC PARAMETERS FOR PSEUDOFIRST-ORDER, PSEUDOSECOND-ORDER, INTRAPARTICLE DIFFUSION, AND CHRASTIL'S DIFFUSION MODEL (SORBENT DOSE 2.0 G/DM^3, TEMPERATURE 25.0°C ± 0.2°C, PH 2.0 ± 0.1)

	Initial DBS concentration (mg/dm^3)									
Parameter	*10*	*20*	*50*	*100*	*200*	*400*	*600*	*800*	*1,000*	*1,200*
q_e, exp (mg/g)	4.98 ± 0.07	9.81 ± 0.15	23.00 ± 0.35	45.23 ± 0.68	97.29 ± 1.46	189.90 ± 2.85	285.41 ± 4.28	377.16 ± 5.66	428.78 ± 6.43	454.82 ± 6.82
Pseudofirst-order nonlinear regression										
q_e, cal (mg/g)	4.92 ± 0.07	9.68 ± 0.15	22.67 ± 0.34	44.63 ± 0.70	93.67 ± 1.41	186.63 ± 2.80	274.95 ± 4.12	360.78 ± 5.41	380.06 ± 5.70	401.61 ± 6.02
k_1 (min^{-1})	0.37	0.24	0.24	0.13	0.07	0.03	0.02	0.01	0.01	0.01
r^2	0.978	0.987	0.987	0.991	0.984	0.995	0.994	0.987	0.975	0.968
Pseudosecond-order nonlinear regression										
q_e, cal (mg/g)	5.06 ± 0.08	9.98 ± 0.15	23.27 ± 0.35	46.37 ± 0.70	98.38 ± 1.48	199.94 ± 3.00	302.32 ± 4.53	409.35 ± 6.13	435.41 ± 6.53	462.62 ± 6.94
k_2 (g mg-1 min-1)	0.104	0.031	0.016	0.004	9×10^{-4}	2×10^{-4}	8×10^{-5}	3×10^{-5}	3×10^{-5}	2×10^{-5}
r^2	0.990	0.996	0.997	0.997	0.997	0.998	0.997	0.993	0.989	0.984
Intraparticle diffusion model										
k_{i1} (mg/[g·min$^{1/2}$])	1.87	3.14	6.25	10.86	15.93	21.49	22.67	23.00	23.57	23.90
C_1 (mg/g)	0.255	0.587	0.636	0.694	0.751	0.799	0.830	0.836	0.878	0.880
r^2	0.853	0.924	0.980	0.955	0.971	0.981	0.996	0.996	0.992	0.992
k_{i2} (mg/[g·min$^{1/2}$])	0.170	0.362	0.400	1.302	1.536	2.29	4.97	5.08	5.11	5.10
C_2 (mg/g)	3.87	6.08	19.54	32.85	70.28	99.74	183.4	252.3	300.3	304.3
r^2	0.892	0.935	0.980	0.908	0.972	0.980	0.961	0.984	0.993	0.938
k_{i3} (mg/[g·min$^{1/2}$])	2×10^{-4}	1×10^{-3}	8×10^{-3}	9×10^{-3}	0.020	0.121	0.430	0.486	—	—
C_3 (mg/g)	4.97	9.77	22.75	45.20	96.66	185.9	269.2	358.7	—	—
r^2	0.659	0.352	0.348	0.750	0.197	0.590	0.982	0.988	—	—
Chrastil's diffusion model										
q_e, cal (mg/g)	4.92 ± 0.07	9.74 ± 0.15	22.81 ± 0.34	44.80 ± 0.67	94.54 ± 1.42	187.81 ± 2.81	279.06 ± 4.19	377.95 ± 5.70	414.11 ± 6.21	449.43 ± 6.74
k_C	0.162	0.075	0.068	0.051	0.018	0.010	6×10^{-3}	3×10^{-3}	2×10^{-3}	1×10^{-3}
n	0.925	0.720	0.624	0.832	0.627	0.724	0.691	0.594	0.517	0.502
r^2	0.977	0.990	0.996	0.994	0.988	0.998	0.999	0.999	0.996	0.997

DBS, sodium dodecylbenzenesulfonate.

seen from the data presented in Table 2, the determination coefficients for the pseudofirst-order kinetics obtained by nonlinear analysis are relatively high for all studied initial DBS concentrations. Likewise, the determined values of q_e calculated from the Lagergren's equation showed similarity with the experimental values, which indicated that pseudofirst-order kinetics can predict the sorption of DBS onto LVB-Al_2O_3.

Pseudosecond-order model. Pseudosecond-order kinetic model (Ho and McKay, 1998), based on equilibrium sorption, can be expressed as follows:

$$\frac{dq}{dt} = k_1(q_e - q_t)^2 \tag{5}$$

Integrating the previous equation for boundary conditions $t=0$ to $t=t$ and $q_t=0$ to $q_t=q_t$ gives the following:

$$q_t = \frac{q_e^2 k_2 t}{1 + k_2 q_e t} \tag{6}$$

where k_2 (g/[mg·min]) is the second-order rate constant, q_e (mg/g) is the amount of sorbate sorbed at equilibrium, q_t (mg/g) is the amount of sorbate sorbed at time t. Plot of q_t versus t for different initial DBS concentrations is shown in Fig. 4 in Supplementary Data.

The values for the pseudosecond-order constant, k_2, and the amount of DBS sorbed at equilibrium, q_e, determined by nonlinear regression, for the sorption of different initial DBS concentrations, are listed in Table 2.

The experimental data showed that the pseudosecond-order model better fitted experimental data than the pseudofirst-order model, due to a higher determination coefficient obtained in all cases. The calculated q_e values for DBS were also relatively close to the experimental q_e values suggesting that the biosorption of DBS by LVB-Al_2O_3 approximately follows a pseudosecond-order reaction. With increasing initial DBS concentration from 10 up to 1,200 mg/g, the pseudosecond-order rate constant, k_2, decreased from 0.104 to 0.00002 g/[mg·min]. At a lower initial DBS concentration, almost all binding sites were free, which resulted in high pseudosecond-order rate constant, while at a higher DBS concentration, saturation of sorption sites occurred and the value of k_2 decreased.

Equilibrium sorption capacity, q_e, calculated by nonlinear regression, increased almost linearly from 5.06 ± 0.07 mg/g up to 409.37 ± 6.14 mg/g with an increase in initial DBS concentration from 10 mg/dm^3 to 800 mg/dm^3, and slightly to 462.65 ± 6.94 mg/g, with a further increase in initial DBS concentration up to 1,200 mg/g. This can also be related to the saturation of binding sites on sorbent surface. Obtained results indicate that the pseudosecond-order model can be successfully used for the study of DBS sorption by LVB-Al_2O_3 and suggest that the mechanism may be presented as a surface reaction, through sharing or exchange of electrons between sorbent and sorbate (Pal *et al.*, 2013; Lee *et al.*, 2016).

Intraparticle diffusion model. Adsorbate transport from the solution phase to the surface of the adsorbent particles occurs in several steps: bulk diffusion, external (film) diffusion, intraparticle diffusion, and finally, sorption of the sorbate onto the sorbent surface. The overall sorption process may be controlled by either one or more steps.

The possibility of intraparticle diffusion was explored by using the intraparticle diffusion kinetics model (Weber Jr. and Morris, 1964), which can be represented by the following equation:

$$q_t = k_d t^{1/2} + C \tag{7}$$

where C is the intercept, and k_{id} is the intraparticle diffusion rate constant (mg/[g·min$^{1/2}$]) determined from a plot q_t versus $t^{1/2}$. If this plot satisfies the linear relationship with the experimental data, then the intraparticle diffusion is a rate-controlling step; if the data exhibit multilinear plots, then some degree of boundary layer control might be present and two or more steps influence the sorption process. The values of C provide an idea about the thickness of the boundary layer: the larger the intercept, the greater the boundary layer effect (Mitic-Stojanovic *et al.*, 2012).

Regression of q_t versus $t^{1/2}$ for the sorption of DBS onto LVB-Al_2O_3 is not linear, suggesting that the intraparticle diffusion is not the only rate-controlling step. The intraparticle diffusion model for all studied initial DBS concentrations showed multilinearity and three stages in sorption, except for initial DBS concentrations of 1,000 and 1,200 mg/dm^3, where two stages in sorption were obtained. Plots of q_t versus $t^{1/2}$ for different initial DBS concentrations are shown in Fig. 5 in Supplementary Data. Similar results were shown in the studies of Cheung *et al.* (2007) and Allen *et al.* (1989), where authors fitted kinetic data by three linear lines with a different slope.

The first, sharper portion of the plot can be attributed to the diffusion of DBS through the solution to the external surface of the sorbent, or the boundary layer diffusion of solute molecules. It is a rate-limiting process at the beginning of the sorption. The second portion described the gradual sorption stage, where intraparticle diffusion was rate limiting. The third portion was attributed to the final equilibrium stage for which the intraparticle diffusion started to slow down due to the extremely low DBS concentration left in the solution.

It could be deduced that there were three processes that controlled the rate of molecules sorption but only one was rate limiting in any particular time range. The slope of the linear portion indicated the rate of the sorption. The lower slope corresponded to a slower sorption process. One could observe that the diffusion in the bulk phase to the exterior surface of adsorbent, which started at the onset of the process, was the fastest. The second portion of the plot seemed to refer to the diffusion into mesopores, and the third one, with the lowest slope, to sorption into micropores. This implies that the intraparticle diffusion of DBS molecules into micropores was the rate-limiting step in the sorption process on LVB-Al_2O_3, particularly over long contact time periods.

The value of rate constant for intraparticle diffusion k_{id1} and k_{id2} shown in Table 2 increases with increasing initial DBS concentration. Increasing the constant for intraparticle diffusion k_{id1} and k_{id2} indicates a greater driving force with increasing initial DBS concentration (bulk liquid concentration raises the driving force of DBS to transfer from the bulk solution onto and into the solid particle). Based on k_{id1} and

k_{id2} values, it can be concluded that film diffusion is more efficient than intraparticle diffusion.

In addition, the C_1 and C_2 (thickness of the boundary layer) values varied like the k_{id} values with the initial DBS concentration (Table 2) indicating film diffusion in the rate-limiting step. A larger C value corresponds to a greater boundary layer diffusion effect.

The intraparticle diffusion rate constant, k_{i3}, was determined from the slope of the third portion of the plot, while increment represents constant C. The calculated intraparticle diffusion rate constants (Table 2) increased from 2.7×10^{-4} to 0.486 mg/[g·min$^{1/2}$] with increasing initial DBS concentration from 10 to 800 mg/dm^3, which can be related to faster diffusion, thus also biosorption, because a higher initial DBS concentration produces a stronger driving force for diffusion. In addition, constant C_3, which is taken to be proportional to the extent of boundary layer thickness, increased from 4.97 to 358.77 by increasing initial DBS concentration, indicating decreases in the rate of the external mass transfer and hence increases in the rate of internal mass transfer.

The determination coefficients for the intraparticle diffusion model are slightly lower than those of the pseudosecond-order kinetic model.

Chrastil's diffusion model. Chrastil's diffusion model describes sorption kinetics in diffusion-controlled systems. The model can be expressed by the following equation (Chrastil, 1990):

$$q_t = q_e\left(1 - e^{-k_C A_0 t}\right)^n \tag{8}$$

where k_C is a rate constant (dm^3/[g·min]), which depends on diffusion coefficients and the sorption capacity of biosorbent, A_0 is the dose of biosorbent (g/dm^3), and n is a heterogeneous structural diffusion resistance constant, which can range from 0 to 1. Constant n is independent of the sorbate concentration, sorbent concentration A_0, q_e, and temperature (Chrastil, 1990; Mitic-Stojanovic *et al.*, 2012). In systems with small diffusion resistance, parameter n approximates 1, while the more significant resistance parameter n assumes small values (<0.5). The plot of q_t versus t for different initial DBS concentrations is shown in Fig. 6 in Supplementary Data.

Parameters of the model, q_e, k_C, and n, for the sorption of DBS at initial concentration from 10 up to 1,200 mg/dm^3 were determined by a nonlinear regression analysis of experimental data according to Equation (8) and given in Table 2.

Obtained high determination coefficients, larger than 0.98 (Table 2), indicate a very good fit of experimental kinetic data with Chrastil's model, for all tested concentrations (10–1,200 mg/dm^3). Applicability of this diffusion model also confirms similar values of the calculated q_e with experimentally determined q_e (Table 2). The results obtained for the diffusion resistance coefficient show values between 0.925 and 0.502 (Table 2) for initial DBS concentration from 10 up to 1,200 mg/dm^3, indicating that the sorption process of DBS on LVB-Al_2O_3 is significantly limited by diffusion resistance.

Adsorption isotherm

Sorption isotherms represent the distribution of sorbate between the biosorbent and solution, when the system is at equilibrium. Isotherm studies provide information important for the optimization of the biosorption mechanism pathways, expression of the surface properties, capacities of biosorbents, and effective design of the biosorption systems. In this study, the experimental data were analyzed by using the following equilibrium models: Langmuir, Freundlich, and Dubinin–Radushkevich (D-R).

Langmuir isotherm model

The Langmuir model assumes that the uptake of adsorbate occurs on a homogeneous surface by monolayer adsorption without any interaction between adsorbed species (Langmuir, 1918; Ho and McKay, 2000). The nonlinear form of Langmuir isotherm can be presented by the following equation:

$$q_e = \frac{q_m K_L c_e}{1 + K_L c_e} \tag{9}$$

where q_e is the amount of sorbate sorbed at equilibrium (mg/g), c_e is the equilibrium concentration of the sorbate in solution (mg/dm^3), q_m is the maximum sorption capacity (mg/g), and K_L is a Langmuir constant related to the energy of sorption, reflecting quantitatively the affinity between the sorbate and the sorbent. Maximum sorbate uptake q_m and Langmuir constant K_L can be deduced from experimental data by a nonlinear regression of the plot q_e versus c_e (Fig. 7 in Supplementary Data) and they are presented in Table 3.

The high value of determination coefficient suggests that the Langmuir isotherm provides a good model of the sorption DBS onto LVB-Al_2O_3. The monolayer maximum DBS uptake capacity, q_m, estimated from Langmuir model is 513.28 ± 7.70 mg/g, and the experimental value is 454.89 ± 6.82 mg/g. The Langmuir isotherm model makes it possible to predict if a sorption system is favorable or unfavorable by calculating R_L, a dimensionless constant referred to as the equilibrium parameter using the following equation:

$$R_L = \frac{1}{1 + K_L c_0} \tag{10}$$

where K_L (dm^3/mg) refers to the Langmuir constant and c_0 is denoted as the initial sorbate concentration (mg/dm^3). R_L value indicates the sorption nature to be unfavorable ($R_L > 1$), linear ($R_L = 1$), favorable ($0 < R_L < 1$), or irreversible ($R_L = 0$).

Calculated values of R_L for the initial DBS concentrations from 10 mg/dm^3 up to 1,200 mg/dm^3 spanned the range from

Table 3. Parameters of Sorption Isotherm Models for DBS Sorption onto LVB-Al_2O_3

Adsorption isotherm	*Parameters*	*Values*
Langmuir	K_L (dm^3/mg)	0.038 ± 0.001
	q_m (mg/g)	513.28 ± 7.70
	R^2	0.980
Freundlich	K_F, (mg/g)$^{1/n}$	66.65 ± 0.99
	n	2.76 ± 0.04
	R^2	0.877
Dubinin–Radushkevich	q_{DR}	446.48 ± 6.70
	K_{DR}	3.038×10^{-7}
	E (J/mol)	1285.70
	R^2	0.952

0.787 to 0.030, confirming the favorability of the present process. Although the sorption process is favorable over the entire studied initial concentration range, it is more favorable at higher initial DBS concentrations than at lower ones.

Freundlich isotherm model

The Freundlich empirical adsorption isotherm equation is based on adsorption on a heterogeneous surface. It is assumed that the stronger binding sites are occupied first and that the binding strength decreases with the increasing degree of site occupation (Freundlich, 1906). The nonlinear form of this isotherm can be presented by the following equation:

$$q_e = K_f c_{eq}^{1/n} \tag{11}$$

where q_{eq} is the amount of sorbate sorbed at equilibrium (mg/g), c_{eq} is the equilibrium concentration of sorbate in solution (mg/dm^3), K_F is Freundlich constant, related to the sorption capacity, and $1/n$ is Freundlich exponent, related to the intensity of sorption, varying with the heterogeneity of the sorbent surface. When $1/n = 1$, free energy for all sorbate concentrations is constant; when $1/n < 1$, sorbate is added with weaker and weaker free energies, and finally, when $1/n > 1$, more sorbate presence in the sorbent enhances the free energies of further sorption (Schwarzenbach *et al.*, 2003). The Freundlich isotherm for the sorption of DBS on LVB-Al_2O_3 is shown in Fig. 7 in Supplementary Data.

Experimental data for DBS sorption indicate favorable sorption, which is in accordance with determined n value of 2.76. However, the low determination coefficient value ($R^2 = 0.877$) confirmed that the Freundlich model was not suitable for predicting sorption of DBS onto LVB-Al_2O_3 from aqueous solution (Aguayo-Villarreal *et al.*, 2013).

D-R isotherm model

The D-R model is an empirical model developed for the sorption of subcritical vapors in micropore solids, where the sorption process follows a pore filling mechanism onto an energetically nonuniform surface (Dubinin and Radushkevich, 1947). So, the D-R isotherm is an analog of Langmuir type but it is more general because it does not assume a homogeneous surface or constant sorption potential. The D-R model is given by the following nonlinear equation:

$$q_e = q_{DR} \exp(-K_{DR}\varepsilon^2) \tag{12}$$

where q_{DR} (mg/g) is the Dubinin–Radushkevich model constant representing the theoretical monolayer saturation capacity, K_{DR} (mol^2/kJ^2) is the constant of sorption energy related to mean sorption energy, and ε is the Polanyi potential defined as follows:

$$\varepsilon = RT \ln\left(1 + \frac{1}{c_e}\right) \tag{13}$$

where R, T, and c_e represent the gas constant (8.314 J/[mol·K]), absolute temperature (K), and sorbate equilibrium concentration (mg/dm^3), respectively.

Values q_{DR}, K_{DR}, and E should be determined from the nonlinear plot of q_e versus c_e (Fig. 7 in Supplementary Data). The mean sorption energy, which may provide useful information with regard to whether or not sorption is subject to a chemical or physical process, can be calculated as follows:

$$E = \frac{1}{\sqrt{2K_{DR}}} \tag{14}$$

The value of mean biosorption energy, which is in the range of 1–8 kJ/mol and 9–16 kJ/mol, suggested the physical sorption and chemical sorption or ion exchange, respectively. According to the calculated E value, which was 1285.70 J/mol, physical sorption can be involved in DBS sorption onto LVB-Al_2O_3. Considering determination coefficient value ($R^2 = 0.952$), it can be concluded that the D-R model fits well with experimental data (Table 3).

Conclusion

A new material based on the chemical modification of *L. vulgaris* shell with Al_2O_3 was synthesized to improve ability of starting biomass to remove anionic organic pollutants, such as DBS. Modification of the biosorbent was confirmed by FTIR spectrum analysis. SEM micrographs showed that the chemical modification did not change the biomaterial morphological structure. The EDX analysis shows the presence of carbon and oxygen with aluminum. Based on weight percentage quantification of samples, there is 29.63% of carbon, 52.87% of oxygen, and 17.50% of aluminum in LVB-Al_2O_3 biosorbent. No separate crystalline Al_2O_3 phase was detected in LVB-Al_2O_3 by the XRD pattern, further indicating the chemical bond between Al_2O_3 and the biomaterial functional groups.

The obtained modified biosorbent showed significant sorption improvement in the removal of DBS compared with the starting biomass. The initial pH strongly affects the sorption of DBS onto LVB-Al_2O_3. Complete DBS removal was attained at lower pHs (1–3); as the pH increases up to 9, DBS removal rapidly decreases. It can be assumed that the main binding mechanism is ionic exchange, based on the attraction between the negatively charged sulfonic group of DBS and the positively charged sorbent surface. However, at higher pH values, the material has adsorbed a certain amount of DBS as well, indicating that ionic exchange is not the only sorption mechanism, even though it is predominant. The extent DBS removal is directly related to the concentration of LVB-Al_2O_3 in the suspension, with an optimal biosorbent dose of 2.0 g/dm^3.

The sorption process followed the pseudosecond-order model, indicating that surface reaction is the rate-limiting step that controls the sorption. The sorption process can also be well described by the three-stage intraparticle and Chrastil's diffusion model, indicating that both reaction and diffusion processes can be involved in the biosorption of DBS onto LVB-Al_2O_3. The Langmuir isotherm model showed the best fit to experimental data in describing the sorption of DBS on biosorbent. The maximum sorption capacity was 513.28 mg DBS per g of LVB-Al_2O_3. In addition to the high RE, LVB-Al_2O_3 possesses other benefits, such as mechanical stability, ease of synthesis, cost-effectiveness, biocompatibility, and environmental friendliness, all of which make it a promising material for the removal of anionic pollutants from water.

Acknowledgment

This work was financed by the Serbian Ministry of Education, Science and Technological Development through Grant No TR34008.

Author Disclosure Statement

No competing financial interests exist.

References

Abdolali, A., Guo, W.S., Ngo, H.H., Chen, S.S., Nguyen, N.C., and Tung, K.L. (2014). Typical lignocellulosic wastes and by-products for biosorption process in water and wastewater treatment: A critical review. *Bioresour. Technol.* 160, 57.

Aguayo-Villarreal, I.A., Ramírez-Montoya, L.A., Hernández-Montoya, V., Bonilla-Petriciolet, A., Montes-Morán, M.A., and Ramírez-López, E.M. (2013). Sorption mechanism of anionic dyes on pecan nut shells (*Carya illinoinensis*) using batch and continuous systems. *Ind. Crops Prod.* 48, 89.

Albadarin, A.B., Solomon, S., Kurniawan, T.A., Mangwandi, C., and Walker, G. (2017). Single, simultaneous and consecutive biosorption of Cr(VI) and Orange II onto chemically modified masau stones. *J. Environ. Manage.* 204, 365.

Allen, S.J., McKay, G., and Khader, K.Y.H. (1989). Intraparticle diffusion of a basic dye during adsorption onto sphagnum peat. *Environ. Pollut.* 56, 39.

Bakircioglu, Y., Bakircioglu, D., and Akman, S. (2010). Biosorption of lead by filamentous fungal biomass-loaded TiO_2 nanoparticles. *J. Hazard. Mater.* 178, 1015.

Beltrán-Heredia, J., Sánchez-Martín, J., and Barrado-Moreno, M. (2012). Long-chain anionic surfactants in aqueous solution. Removal by *Moringa oleifera* coagulant. *Chem. Eng. J.* 180, 128.

Benítez-Guerrero, M., Pérez-Maqueda, L.A., Sánchez-Jiménez, P.E., and Pascual-Cosp, J. (2014). Characterization of thermally stable gamma alumina fibres biomimicking sisal. *Micropor. Mesopor. Mat.* 185, 167.

Bhatnagar, A., Sillanpää, M., and Witek-Krowiak, A. (2015). Agricultural waste peels as versatile biomass for water purification—A review. *Chem. Eng. J.* 270, 244.

Boehm, H.P. (1966). Chemical identification of surface groups. *Adv. Catal.* 16, 179.

Bozbas, S.K., and Boz, Y. (2016). Low-cost biosorbent: *Anadara inaequivalvis* shells for removal of Pb(II) and Cu(II) from aqueous solution. *Process Saf. Environ. Prot.* 103, 144.

Cheung, W.H., Szeto, Y.S., and McKay, G. (2007). Intraparticle diffusion processes during acid dye adsorption onto chitosan. *Bioresour. Technol.* 98, 2897.

Chrastil, J. (1990). Adsorption of direct dyes on cotton: Kinetics of dyeing from finite baths based on new information. *Text. Res. J.* 60, 413.

Copello, G.J., Mebert, A.M., Raineri, M., Pesenti, M.P., and Diaz, L.E. (2011). Removal of dyes from water using chitosan hydrogel/SiO_2 and chitin hydrogel/SiO_2 hybrid materials obtained by the sol–gel method. *J. Hazard. Mater.* 186, 932.

Cserháti, T., Forgács, E., and Orosb, G. (2002). Biological activity and environmental impact of anionic surfactants. *Environ. Int.* 28, 337.

De Quadros Melo, D., De Oliveira Sousa Neto, V., De Freitas Barros, F.C., Raulino, G.S.C., Vidal, C.B., and Do Nascimento, R.F. (2016). Chemical modifications of lignocellulosic materials and their application for removal of cations and anions from aqueous solutions. *J. Appl. Polym. Sci.* 133, 43286.

Dubinin, M.M., and Radushkevich, L.V. (1947). Equation of the characteristic curve of activated charcoal. Proceedings of the USSR Academy of Sciences. *Phys. Chem. Sect*. 55, 331.

Eaton, A.D., Clesceri, L.S., Greenberg, A.E., and Franson, M.A.H. (1998). *Standard Methods for the Examination of Water and Wastewater*, twentieth ed. Washington, DC: American Public Health Association.

Elanthikkal, S., Gopalakrishnapanicker, U., Varghese, S., and Guthrie, J.T. (2010). Cellulose microfibers produced from banana plant wastes: Isolation and characterization. *Carbohydr. Polym.* 80, 852.

El-Sakhawy, M. (2001). Characterization of modified oxycellulose. *J. Therm. Anal. Cal.* 63, 549.

Freundlich, H.M.F. (1906). Over the adsorption in solution. *J. Phys. Chem.* 57, 385.

George, A.L., and White, G.F. (1999). Optimization of the methylene blue assay for anionic surfactants added to estuarine and marine water. *Environ. Toxicol. Chem.* 18, 2232.

Guerrero-Coronilla, I., Morales-Barrera, L., and Cristiani-Urbina, E. (2015) Kinetic, isotherm and thermodynamic studies of amaranth dye biosorption from aqueous solution onto water hyacinth leaves. *J. Environ. Manage.* 152, 99.

Goertzen, S.L., Thériault, K.D., Oickle, A.M., Tarasuk, A.C., and Andreas, H.A. (2010). Standardization of the Boehm titration. Part I. CO_2 expulsion and endpoint determination. *Carbon* 48, 1252.

Ho, Y.S., and McKay, G. (1998). Kinetic models for the sorption of dye from aqueous solution by wood. *Process Saf. Environ. Prot.* 76, 183.

Ho, Y.S., and McKay, G. (2000). The kinetics of sorption of divalent metal ions onto sphagnum moss peat. *Water Res.* 34, 735.

Jardak, K., Drogui, P., and Daghrir, R. (2016). Surfactants in aquatic and terrestrial environment: Occurrence, behavior, and treatment processes. *Environ. Sci. Pollut. Res.* 23, 3195.

Khan, M.N., and Zareen, U. (2006). Sand sorption process for the removal of sodium dodecyl sulfate (anionic surfactant) from water, *J. Hazard. Mater.* 133, 269.

Kosswig, K. (2006). *Ullmann's Encyclopedia of Industrial Chemistry*, seventh ed. Weinheim, Germany: Wiley-VCH.

Kostić, M., Radović, M., Mitrović, J., Antonijević, M., Bojić, D., Petrović, M., and Bojić, A. (2014). Using xanthated *Lagenaria vulgaris* shell biosorbent for removal of Pb(II) ions from wastewater. *J. Iran. Chem. Soc.* 11, 565.

Kumar, P.M., Balasubramanian, C., Sali, N.D., Bhoraskar, S.V., Rohatgi, V.K., and Badrinarayanan, S. (1999). Nanophase alumina synthesis in thermal arc plasma and characterization: Correlation to gas-phase studies. *Mater. Sci. Eng. B* 63, 215.

Kumar, R., Sharma, R.K., and Singh, A.P. (2017). Cellulose based grafted biosorbents—Journey from lignocellulose biomass to toxic metal ions sorption applications—A review. *J. Mol. Liq.* 232, 62.

Lagergren, S. (1898). About the theory of so-called adsorption of soluble substances. *K. vet. akad. handl.* 24, 1.

Landry, C.C., Papp, N., Mason, M.R., Apblett, A.W., Tyler, A.N., MacInnes, A.N., and Barron, A.R. (1995). From minerals to materials: Synthesis of alumoxanes from the reaction of boehmite with carboxylic acids. *J. Mater. Chem.* 5, 331.

Langmuir, I. (1918). The adsorption of gases on plane surfaces of glass, mica and platinum. *J. Am. Chem. Soc.* 40, 1361.

Lee, H., Shim, E., Yun, H.-S., Park, Y.-T., Kim, D., Ji, M.-K., Kim, C.-K., Shin, W.-S., and Choi, J. (2016). Biosorption of Cu(II) by immobilized microalgae using silica: Kinetic, equilibrium, and thermodynamic study. *Environ. Sci. Pollut. Res.* 23, 1025.

Lewis, M.A. (1991). Chronic and sublethal toxicities of surfactants to aquatic animals: A review and risk assessment. *Water Res.* 25, 101.

Liu, B., Wang, D., Li, H., Xu, Y., and Zhang, L. (2011). As(III) removal from aqueous solution using α-Fe2O3 impregnated chitosan beads with As(III) as imprinted ions. *Desalination* 272, 286.

Liu, Y., Liao, T., He, Z., Li, T., Wang, H., Hu, X., Guo, Y., and He, Y. (2013). Biosorption of copper(II) from aqueous solution by Bacillus subtilis cells immobilized into chitosan beads. *Trans. Nonferrous Met. Soc. China.* 23, 1804.

Mahmoodi, N.M., Hayati, B., Arami, M., and Bahrami, H. (2011). Preparation, characterization and dye adsorption properties of biocompatible composite (alginate/titania nanoparticle). *Desalination* 275, 93.

Mitic-Stojanovic, D.-L., Bojic, D., Mitrovic, J., Andjelkovic, T., Radovic, M., and Bojic, A. (2012). Equilibrium and kinetic studies of Pb(II), Cd(II) and Zn(II) sorption by *Lagenaria vulgaris* shell. *Chem. Ind. Chem. Eng. Q.* 18, 563.

Mitic-Stojanovic, D.-L., Zarubica, A., Purenovic, M., Bojic, D., Andjelkovic, T., and Bojic, A.L. (2011). Biosorptive removal of Pb^{2+}, Cd^{2+} and Zn^{2+} ions from water by *Lagenaria vulgaris* shell. *Water SA* 37, 1.

Mösche, M., and Meyer, U. (2002). Toxicity of linear alkylbenzene sulfonate in anaerobic digestion: Influence of exposure time. *Water Res.* 36, 3253.

Pal, A., Pan, S., and Saha, S. (2013). Synergistically improved adsorption of anionic surfactant and crystal violet on chitosan hydrogel beads. *Chem. Eng. J.* 217, 426.

Roberts, J.D., and Caserio, M.C. (1977). *Basic Principles of Organic Chemistry*, second ed. Menlo Park, CA: W. A. Benjamin Incorporation.

Rosen, M.J., and Kunjappu, J.T. (2012). *Surfactants and Interfacial Phenomena, fourth ed.* Hoboken, NJ: John Wiley and Sons.

Schwarzenbach, R.P., Gschwend, P.M., and Imboden, D.M. (2003). *Environmental Organic Chemistry*, second ed. Hoboken, NJ: John Wiley and Sons.

Shah, B.N., Seth, A.K., and Desai, R.V. (2010). Phytopharmacological profile of *Lagenaria siceraria*: A review. *Asian J. Plant Sci.* 9, 152.

Stanković, M.N., Krstić, N.S., Slipper, I.J., Mitrović, J.Z., Radović, M.D., Bojić, D.V., and Bojić, A.L. (2013). Chemically modified *Lagenaria vulgaris* as a biosorbent for the removal of Cu(II) from water. *Aust. J. Chem.* 66, 227.

Tural, B., Ertaş, E., Enez, B., Fincan, S.A., and Tural, S. (2017). Preparation and characterization of a novel magnetic biosorbent functionalized with biomass of *Bacillus subtilis*: Kinetic and isotherm studies of biosorption processes in the removal of methylene blue. *J. Environ. Chem. Eng.* 5, 4795.

Van den Brand, J., Blajiev, O., Beentjes, P.C.J., Terryn, H., and de Wit, J.H.W. (2004). Interaction of anhydride and carboxylic acid compounds with aluminum oxide surfaces studied using infrared reflection absorption spectroscopy, *Langmuir* 20, 6308.

Weber, W.J., Jr., and Morris, J.C. (1964). Kinetics of adsorption on carbon from solution. *J. Sanit. Eng. Div.* 89, 31.

Yang, Y., Chun, Y., Sheng, G., and Huang, M. (2004). pH-dependence of pesticide adsorption by wheat-residue-derived black carbon. *Langmuir* 20, 6736.

Ying, G.-G. (2006). Fate, behavior and effects of surfactants and their degradation products in the environment. *Environ. Int.* 32, 417.